

UPDATES TO THE OPERATING MODEL UNCERTAINTY GRID FOR THE NORTH ATLANTIC SWORDFISH MSE

Adrian Hordyk¹, Michael Schirripa², and Daniela Rosa^{3,4}

SUMMARY

The operating model (OM) uncertainty grid for the management strategy evaluation (MSE) of the North Atlantic Swordfish fishery has been updated. The revised grid has six axes of uncertainty, with 2-3 levels within each axis, for a total of 216 OMs. This paper reports the convergence diagnostics of the 216 OMs and summarizes how the predicted stock dynamics and estimated stock status are influenced by the levels within each axis of uncertainty. The results found the three levels of natural mortality (M), three levels of steepness (h), and three alternative weightings of the indices and length composition data had the largest impact on the variability in the estimated stock dynamics. Down-weighting the CPUE indices resulted in markedly higher estimates of stock status, particularly when M and h were in the highest levels. The inclusion of the environmental covariate had very little influence on the predictions. These results can be used by the Swordfish Species Working Group to evaluate the suitability of the OM uncertainty grid and determine the final grid that will be used in the testing of candidate management procedures.

KEYWORDS

Management Strategy Evaluation, Simulation, Fishery management

1 Introduction

The North Atlantic swordfish fishery (hereafter swordfish) is undergoing a management strategy evaluation (MSE) process. A critical component of the MSE approach is the development of operating models (OMs), mathematical models that describe alternative hypotheses of the dynamics of the fishery system. The Swordfish Species Working Group (hereafter the Group) has chosen to use the approach of an OM uncertainty grid, where the key fishery uncertainties are captured by means of alternative levels in several axes of uncertainty.

The first round of OM development built an uncertainty grid around a base-case model centred on the 2017 North Atlantic swordfish stock assessment (Anon., 2017). This OM grid included 7 axes of uncertainty, each with 2 or 3 levels, with a full factorial design resulting in 288 OMs (see Hordyk, 2020 for details). The Commission has requested the Group to ensure that the swordfish MSE framework is capable of evaluating questions relating to the minimum size regulations for the fishery. Consequently, the assessment model used to condition the operating models was modified to explicitly included options for the fleet-specific retention curves and mortality rate of the discarded sub-legal fish (Schirripa & Hordyk, 2020). Given these changes, the OM

¹ Blue Matter Science Ltd, 2150 Bridgman Avenue, North Vancouver, BC, CANADA, V7P2T9 adrian@bluematterscience.com

² NOAA Fisheries, Southeast Fisheries Science Center, 75 Virginia Beach Drive, Miami, FL, 33149 USA. Michael.schirripa@noaa.gov

³ Instituto Português do Mar e da Atmosfera (IPMA, I.P.), Av. 5 de Outubro s/n, 8700-305 Olhão, PORTUGAL daniela.rosa@ipma.pt

⁴ CCMAR – Centro de Ciências do Mar da Universidade do Algarve, Campus de Gambelas, 8005-139 Faro, PORTUGAL

uncertainty grid was re-built with the newly re-conditioned OMs including a discard mortality rate of 88% on the discarded fish (Coelho & Muñoz-Lechuga, 2019).

During this work it was noted that the design of the operating model uncertainty grid could be improved by removing some redundancy from the axes of uncertainty. The previous OM grid had one axis of uncertainty for the assumed coefficient of variation (CV) for the fishery-dependant catch-per-unit-effort (CPUE) indices (two levels: CV = 0.3 and 0.6), and one axis for the effective sample size (ESS) of the length composition data used in the model (two levels: ESS = 2 and 20). It was noted that, as these are the two primary sources of data used in the model fitting, there was redundancy in these two axes. Decreasing the CV of the CPUE indices has the effect of up-weighting the CPUE data relative to the length composition data, which is qualitatively the same as reducing the ESS of the length composition data. The interactions between the two levels in each axis introduces the redundancy and makes it difficult to interpret the axes of uncertainty.

This issue was resolved by modifying the OM uncertainty grid by replacing these two axes of uncertainty with a new axis that explicitly focused on the relative weight of the CPUE and length composition data. The CV of the CPUE indices and the ESS of the length composition were fixed at the values used in the base case model (0.3 and 2 respectively). A new axis of uncertainty was created (CPUE lambda) with three alternative values for the relative weight of the CPUE indices relative to the length composition data. The lambda for the length composition data was fixed at 1. The three levels of CPUE lambda were 0.05, 1, and 20, representing a relative weight of the CPUE indices of 1/20th, equal to, and 20 times the length composition data.

These values were chosen as they represent the extremes of the scenarios: essentially completely down-weighting the CPUE indices so that the model fit is determined entirely by the length composition data, equally weighting the two data sources, and down-weighting the length composition data so that the model fit is determined entirely by the CPUE indices. An analysis was conducted to ensure that this design was essentially equivalent to the reverse situation; that is, fixing the lambda of the CPUE indices at 1 and adjusting the lambda of the length composition data by the same amount (Schirripa et al., 2021)

A second issue noted during the work on revising the OM grid was a potential problem with some of the length composition data used in the model conditioning. A visual inspection of the length composition data from the US, Canada – Late, Japan, and Portugal fleets indicated that the length data for the period after the introduction of the minimum size regulations (1993 – 2017) appeared to be offset by 3 – 4 length bins. Figures demonstrating this potential issue are shown in **Appendix A**. While this issue requires further discussion from the Group, for the purposes of this analysis the affected length composition data have been adjusted as demonstrated in **Appendix A** and the OM conditioning model was used with the adjusted length data.

This paper provides a summary of convergence diagnostics, estimated reference points, and fishery dynamics for the new OM uncertainty grid.

2 Methods

Convergence of the conditioned models was evaluated in the four ways recommended by Carvalho et al. (2021). First, the conditioned operating models were examined for estimated parameters that were within 1% of the specified minimum and maximum bounds. Next, the final gradient of the objective function for each OM was reported. Carvalho et al. (2021) note that although final gradient values should be relatively small (e.g., $\leq 1E-04$), larger gradient values are not necessary indicative of non-convergence. Third, each OM was confirmed that the Hessian matrix was positive definite (i.e., invertible). Finally, the OMs were examined for high correlations (absolute correlation >0.95) between estimated parameters pairs.

The fleet-specific selectivity and retention curves, and the overall selection and retention pattern (aggregated over fleets) was reported.

The marginal impact of each of the six factors on the estimated stock status (spawning biomass (SB) relative to SB at maximum sustainable yield (SB_{MSY}), SB relative to unfisher spawning biomass (SB_0), and fishing mortality (F) relative to F_{MSY}) and biological reference points (MSY (total removals), equilibrium unfisher recruitment (R_0), SB_{MSY} , and SB_0) were summarized as a series of boxplots, with colors indicating the levels within each factor in the OM uncertainty grid. An ANOVA test was conducted to evaluate if there is a significant difference in the estimated mean spawning stock biomass in the most recent year (2017; SB_{2017}) relative to SB_{MSY} across the different levels for each factor.

The estimated stock dynamics and reference points from the OM uncertainty grid were summarized with boxplots, with colors indicating the levels within each factor in the OM uncertainty grid.

3 Results

3.1 Updated Uncertainty Grid

The full factorial design of the six axes of uncertainty resulted in an uncertainty grid with 216 OMs (**Table 1**).

3.2 Convergence Diagnostics

70 of the 216 OM (32%) had at least one parameter close to the specified bounds, with the majority (67) having 1 parameter close the bounds and 3 OMs having 2 parameters close to bounds. The four parameters that were close to the bounds were all related to the estimated selectivity curves for two fleets (Japan – Mid and US; **Table 2**), the majority (61) of which were related to the descending limb of the selectivity curve for the US fleet.

Most of the OMs had a very small gradient value (< 0.0001). 99 OMs had a gradient value larger than the recommended cut-off value (0.0001) and 16 OMs had a gradient value > 0.01 . Operating model #203 had the largest gradient value of 0.05 (**Figure 1**).

All 216 operating models had a positive definite Hessian matrix.

130 OMs had absolute correlation > 0.95 between estimated parameter pairs. The high correlations occurred in 21 parameter pairs, predominantly between pairs of selectivity parameters for a given fleet, and between the fleet-specific catchability coefficients and the estimate of virgin recruitment (R_0 ; **Table 3**).

3.3 Selectivity and Retention Curves

The shape of the estimated selectivity curves varied between the operating models, especially for the Spain, US, Japan – Early, Japan – Late and Portugal fleets when the length composition data were down-weighted relative to the CPUE indices (CPUE lambda = 20; **Figure 2**).

The overall selectivity and retention patterns were calculated as a weighted average of the fleet-specific curves (weighted by fleet-specific fishing mortality). The ascending limb of the selectivity curves began around 60 cm and included a wide-range of dome-shaped patterns (**Figure 3**). Discard mortality of 88% was assumed for all fish selected by the fishing gear that were at lengths below the retention curve.

3.4 Estimated Stock Status and Biological Reference Points

The mean estimated SB/SB_{MSY} over the whole grid was 1.56 (SD = 1.26), with median value of 1.04 and minimum and maximum values of 0.546 and 6.12. The mean estimated F/F_{MSY} over the whole grid was 1.04 (SD = 0.628), with median value of 1.01 and minimum and maximum values of 0.054 and 2.44.

Table 4 shows the mean and standard deviation of the estimated SB/SB_{MSY} , F/F_{MSY} , and depletion (SB/SB_0) in 2017 for the levels within each of the 6 axes of uncertainty. A one-way analysis of variance (ANOVA) detected no significant difference ($P > 0.05$) in the mean values of SB/SB_{MSY} , F/F_{MSY} , and SB/SB_0 for the two levels of recruitment variability and the two levels of the environmental covariate (**Table 4**). The estimates of depletion were almost identical for the three levels of steepness (**Table 4**). No significant difference in mean SB/SB_{MSY} was detected for the two levels of the increase in catchability (**Table 4**).

Boxplots of the relative stock status (SB/SB_{MSY} , SB/SB_0 , and F/F_{MSY}) as well as the absolute estimates of MSY , R_0 , SB_{MSY} , and SB_0 are shown for natural mortality (**Figure 4**) recruitment variability (**Figure 5**), steepness (**Figure 6**), CPUE lambda (**Figure 7**), increase in catchability (**Figure 8**), and the environmental covariate (**Figure 9**).

Increasing values of natural mortality (M) resulted in higher estimates of stock status (lower fishing mortality), higher estimates of MSY and SB_{MSY} , and lower estimates of unfished recruitment (R_0) and spawning biomass (SB_0) (**Figure 4**). There was a considerable increase in the variability of the estimates of SB/SB_{MSY} , F/F_{MSY} , SB_{MSY} , and SB_0 for the OMs where natural mortality was 0.3 (**Figure 4**).

There was very little difference in the distributions of estimated stock status and reference points for the two levels of recruitment variability (**Figure 5**), and no significant difference in the mean estimates of stock status between the two levels (**Table 4**).

Increasing values of the steepness parameter had a similar trend to that of the natural mortality rate, with higher values of steepness resulting in more optimistic estimates of stock status and lower estimates of the scaling

parameters R_0 and SB_0 (**Figure 6**). The distributions for MSY and SB_{MSY} were skewed and there was a large amount of variability in the estimates of SB_0 and R_0 across the three levels.

The three alternative relative weightings of the CPUE and length composition data (CPUE lambda) had a significant impact on the estimate stock status and reference points (**Figure 7, Table 4**). Down-weighting the CPUE data (CPUE lambda = 0.05) resulted in increased variability in the estimates of stock status and absolute reference points compared to the OMs where the length composition data was equally weighed (CPUE lambda = 1) and down-weighted (CPUE lambda = 20; **Figure 7**).

There was very little difference in the estimates of absolute reference points for the two levels of the axes that considered the annual 1% increase in catchability (**Figure 8**). However, the estimated stock status was affected by the different assumptions, with the OMs where catchability was assumed to increase by 1% per year resulting in lower estimates of stock status and higher estimates of fishing mortality (**Figure 8**).

Finally, the inclusion of the environmental covariate with the CPUE indices had very little impact on the estimates, with no significant difference in the mean estimates of stock status or the biological reference points (**Figure 9, Table 4**).

3.5 *Bi-Variate Kobe Plots*

Table 4 and the univariate boxplots indicate that three axes have the most impact on the estimated stock dynamics: natural mortality, steepness, and the alternative weightings of the CPUE and length composition data (CPUE lambda). A set of Kobe plots were created for a more detailed look at the OM dynamics within each of the levels in these 3 factors.

For the 72 OMs where the CPUE data was down-weighted (CPUE lambda = 0.05), the terminal estimates of SB/SB_{MSY} were all well above 1 and $F/F_{MSY} < 1$ when $M = 0.3$, and increased as the steepness level increased (**Figure 10**). At the two lower levels of M (0.1 and 0.2) the estimated spawning biomass in 2017 was closer to SB_{MSY} , with the estimates of stock status increasing as the steepness level increased (**Figure 10**).

When the lambdas on the CPUE data and the length composition data were equal (CPUE lambda = 1) the terminal spawning biomass was slightly lower and fishing mortality slightly higher (**Figure 11**). The OMs with high natural mortality (0.3) resulted in the most optimistic estimates of stock status, especially when steepness was also in the higher levels (0.75 and 0.9).

The estimated stock status was less variable in the OMs where the CPUE data was up-weighted (CPUE lambda = 20; **Figure 12**), with the estimates of F/F_{MSY} in the terminal year close to 1, and $SB/SB_{MSY} < 1$ for the lowest level of M (0.1), and distributed around 1 for higher levels of M (0.2 and 0.3) except for when both h and M were at the highest levels (**Figure 12**).

3.6 *OM Diagnostic Plots and Additional Summary Plots*

Additional plots of the OM dynamics, and OM-specific diagnostic plots are available in **Appendix B**.

4 Discussion

The operating model uncertainty grid for the North Atlantic swordfish was updated to include the fleet-specific retention curves and discard mortality of 88% on the sub-legal fish that are selected by the fishing gear, and modified to collapse the previous two axes relating to the CPUE CV and effective sample size of the length compositions into a single axis controlling for the relative weight between these two data sources. Furthermore, the length composition data for some fleets were modified in this analysis to account for an apparent issue with data entry (**Appendix A**).

Replacing the two axes relating to the CV of the CPUE indices and the effective sample size of the length composition data resulted in a grid 25% smaller than the previous uncertainty grid and improves with the interpretation of the axes of uncertainty. However, the estimated stock status from the revised grid are more variable compared to the previous version of the grid, especially for the OMs where the CPUE indices were down-weighted (CPUE lambda = 0.05; **Figure 7**; also compare **Table 4** with **Table 2** in Hordyk (2020)).

Similar to the previous uncertainty grid, several of the fleet selectivity parameters were highly correlated and final estimated values were close to the bounds. Further analysis is required to determine if adjusting the bounds for these parameters would have a significant impact on the estimated stock dynamics. However, it may be

difficult to achieve a grid where the selectivity parameters for some fleets do not hit the lower or upper bounds, as many of the parameters are bounded by the choice of the length bins used in the data.

The results demonstrate that the uncertainty in natural mortality (M), steepness (h), and the alternative weightings of the CPUE and length composition data are most consequential in terms of the predicted stock dynamics. The alternative levels for two of the axes, recruitment variability and the environmental covariate, did not show a significant difference in the mean estimated stock status (**Table 4**). However, further analysis is required to determine if the levels within these axes will have an impact on the performance and choice of candidate management procedures.

The results of the updated grid will be discussed by the Swordfish Species Working Group to decide if further modifications to the grid are required, or if the grid can be adopted for the MSE analyses for the swordfish fishery.

5 Acknowledgements

The Swordfish Species Working Group, particularly Kyle Gillespie, Alex Hanke, and Rui Coelho, are thanked for their input and feedback on this work. D. Rosa is supported by an FCT Doctoral grant (Ref: SFRH/BD/136074/2018) funded by National Funds and the European Social Fund. This work was carried out under the provision of the ICCAT Science Envelope and the ICCAT – EU Grant Agreement – Strengthening the scientific basis for decision-making in ICCAT. The contents of this paper do not necessarily reflect the point of view of ICCAT or other funders and in no ways anticipate ICCAT future policy in this area.

6 References

- Anon. (2017). Report of the 2017 ICCAT Atlantic Swordfish Stock Assessment Session. SCRS/2017/008. *Collect. Vol. Sci. Pap. ICCAT*, 74(3), 841–967.
- Carvalho, F., Winker, H., Courtney, D., Kapur, M., Kell, L., Cardinale, M., Schirripa, M., Kitakado, T., Yemane, D., Piner, K. R., Maunder, M. N., Taylor, I., Wetzel, C. R., Doering, K., Johnson, K. F., & Methot, R. D. (2021). A cookbook for using model diagnostics in integrated stock assessments. *Fisheries Research*, 240, 105959. <https://doi.org/10.1016/j.fishres.2021.105959>
- Coelho, R., & Muñoz-Lechuga, R. (2019). Hooking mortality of swordfish in pelagic longlines: Comments on the efficiency of minimum retention sizes. *Reviews in Fish Biology and Fisheries*, 29(2), 453–463. <https://doi.org/10.1007/s11160-018-9543-0>
- Hordyk, A. (2020). Impact of uncertainty in the North Atlantic swordfish operating models on estimated stock status and relative performance of reference management procedures. *SCRS/2020/155*.
- Schirripa, M., & Hordyk, A. (2020). Migrating the North Atlantic swordfish stock assessment model to an updated version of Stock Synthesis with analysis of the current minimum size regulation. *SCRS/2020/159. Collect. Vol. Sci. Pap. ICCAT*, 77(3), 654–668.
- Schirripa, M., Rosa, D., & Hordyk, A. (2021). An evaluation of data weighting for the ICCAT Northern Swordfish Management Strategy Evaluation, SCRS/2021/098. *Collect. Vol. Sci. Pap. ICCAT*.

7 Tables

Table 1. The six axes of uncertainty (columns) and the levels for each factor (rows) in the operating model (OM) uncertainty grid for the North Atlantic Swordfish MSE. The full factorial design of these factors and levels results in a grid of 216 OMs.

Natural Mortality (M)	Recruitment variability (sigmaR)	Steepness (h)	CPUE Lambda	1% Annual Increase in Catchability	Environmental Covariate
0.1	0.2	0.60	0.05	FALSE	FALSE
0.2	0.6	0.75	1	TRUE	TRUE
0.3		0.90	20		

Table 2. The four parameters in the 70 operating models that were within 1% of the bounds.

Parameter	Number of Operating Models
Size_DblN_descend_se_US_2	61
Size_DblN_peak_JPN_MID_6	7
Size_DblN_ascend_se_US_2	3
Size_DblN_peak_JPN_MID_6	2

Table 3. Mean correlation values between the 21 parameter pairs with absolute correlation > 0.95.

Parameter 1	Parameter 2	Mean Correlation
Size_DblN_end_logit_JPN_ERLY_5(5)	LnQ_base_JPN_ERLY_5(5)	-0.98058
Size_DblN_ascend_se_US_2(2)	Size_DblN_peak_US_2(2)	0.953894
Size_DblN_ascend_se_CAN_LATE_3(3)	Size_DblN_peak_CAN_LATE_3(3)	0.955287
Size_DblN_end_logit_JPN_MID_6(6)	LnQ_base_JPN_MID_6(6)	-0.96993
LnQ_base_Age-5+(16)	SR_LN(R0)	-0.95955
Size_DblN_ascend_se_JPN_MID_6(6)	Size_DblN_peak_JPN_MID_6(6)	0.977236
Size_DblN_descend_se_JPN_MID_6(6)	Size_DblN_peak_JPN_MID_6(6)	-0.98686
Size_DblN_end_logit_PORT_8(8)	LnQ_base_PORT_8(8)	-0.98416
Size_DblN_top_logit_JPN_ERLY_5(5)	Size_DblN_peak_JPN_ERLY_5(5)	-0.98071
Size_DblN_descend_se_JPN_MID_6(6)	LnQ_base_JPN_MID_6(6)	-0.98997
Size_DblN_top_logit_JPN_MID_6(6)	Size_DblN_peak_JPN_MID_6(6)	-0.99718
Main_RecrDev_2015	SR_LN(R0)	0.954681
Size_DblN_ascend_se_JPN_ERLY_5(5)	Size_DblN_peak_JPN_ERLY_5(5)	0.980195
Size_DblN_ascend_se_JPN_ERLY_5(5)	Size_DblN_top_logit_JPN_ERLY_5(5)	-0.97831
LnQ_base_US_2(2)	SR_LN(R0)	-0.96546
LnQ_base_CAN_LATE_3(3)	SR_LN(R0)	-0.95998
LnQ_base_Age-1(12)	SR_LN(R0)	-0.95841
LnQ_base_Age-2(13)	SR_LN(R0)	-0.9612
LnQ_base_Age-3(14)	SR_LN(R0)	-0.971
LnQ_base_Age-4(15)	SR_LN(R0)	-0.96564
LnQ_base_Age-5+(16)	LnQ_base_Age-3(14)	0.953361

Table 4. The mean and standard deviation of the estimated stock status (SB/SB_{MSY} , F/F_{MSY} , and depletion, in 2017) for each factor and level in the 216 operating models in the uncertainty grid for the North Atlantic swordfish. Factors that do not have a significant difference ($P > .05$) in estimated stock status across the levels are indicated with gray shading (ANOVA).

Factor	Level	SB/SB_{MSY}	F/F_{MSY}	Depletion
Natural Mortality (M)	0.1	0.812 (0.158)	1.65 (0.434)	0.215 (0.050)
	0.2	1.20 (0.471)	1.00 (0.362)	0.268(0.071)
	0.3	2.67 (1.62)	0.460 (0.394)	0.529 (0.250)
Recruitment Variability (sigmaR)	0.2	1.64 (1.35)	0.990 (0.585)	0.357 (0.223)
	0.6	1.48 (1.16)	1.08 (0.669)	0.318 (0.184)
Steepness (h)	0.6	1.12 (0.660)	1.26 (0.629)	0.335 (0.184)
	0.75	1.40 (0.95)	1.05 (0.610)	0.333 (0.184)
	0.90	2.17 (1.70)	0.806 (0.569)	0.344 (0.228)
CPUE Lambda	0.05	2.04 (1.64)	1.02 (0.852)	0.429 (0.275)
	1.0	1.67 (1.17)	0.891 (0.497)	0.358 (0.162)
	20	0.974 (0.364)	1.21 (0.414)	0.225 (0.057)
Increase in Catchability	FALSE	1.72 (1.27)	0.893 (0.558)	0.375 (0.20)
	TRUE	1.40 (1.24)	1.18 (0.663)	0.299 (0.203)
Environmental Covariate	FALSE	1.51 (1.20)	1.06 (0.628)	0.327 (0.195)
	TRUE	1.61 (1.32)	1.02 (0.630)	0.348 (0.214)

8 Figures

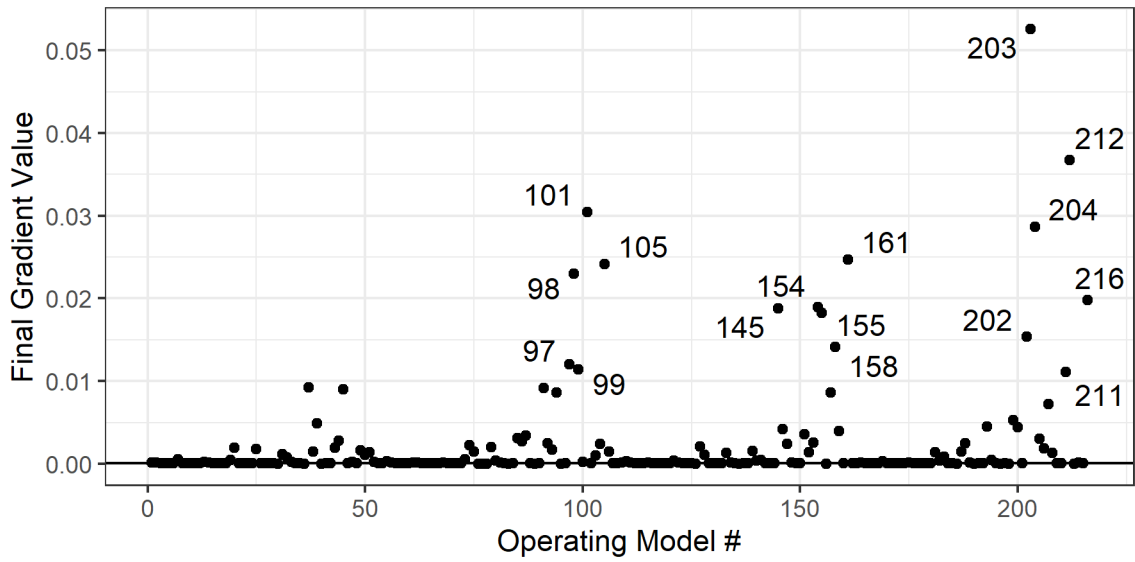


Figure 1. The final gradient values of the 216 operating models. The numbers indicate the operating models with final gradient values > 0.01 .

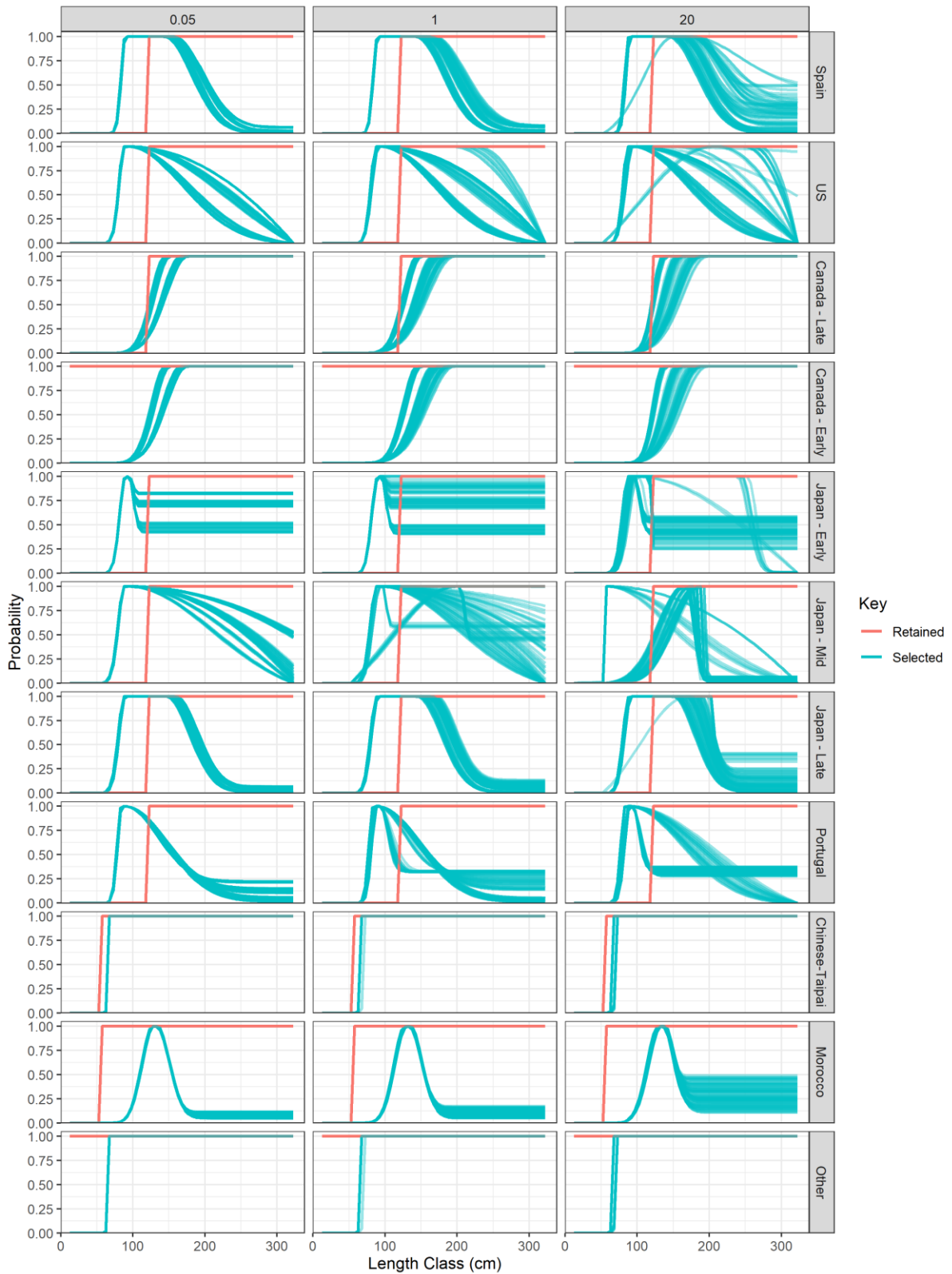


Figure 2. The estimated selectivity (blue) and fixed retention (red) curves in the terminal year (2017) for the 11 fleets (rows) and three level of CPUE lambda (columns) in the 216 operating models in the uncertainty grid for the North Atlantic swordfish.

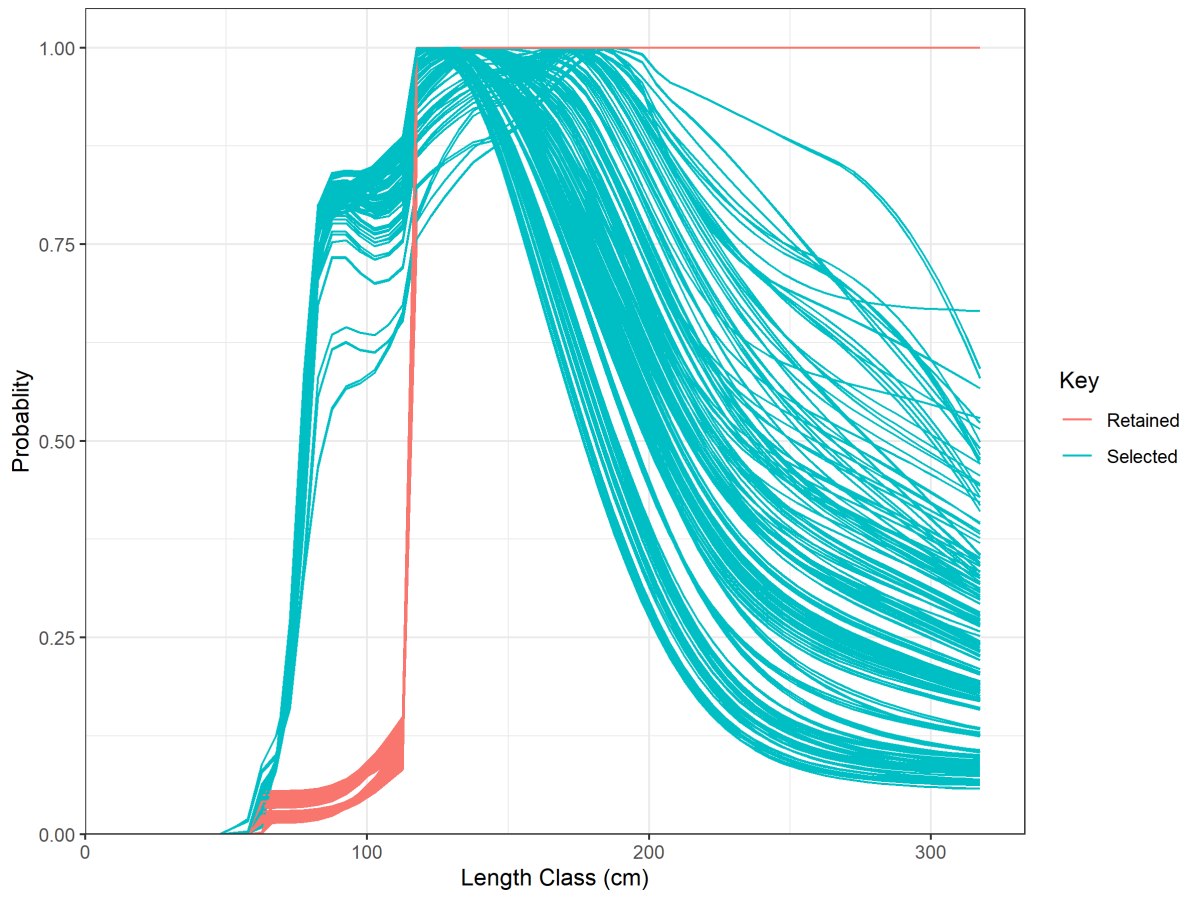


Figure 3. The overall selectivity (blue) and retention (red) curves in the terminal year (2017) for the 216 operating models in the uncertainty grid. The aggregated selectivity pattern was calculated as the average fleet-specific selectivity weighted by the fleet-specific fishing mortality.

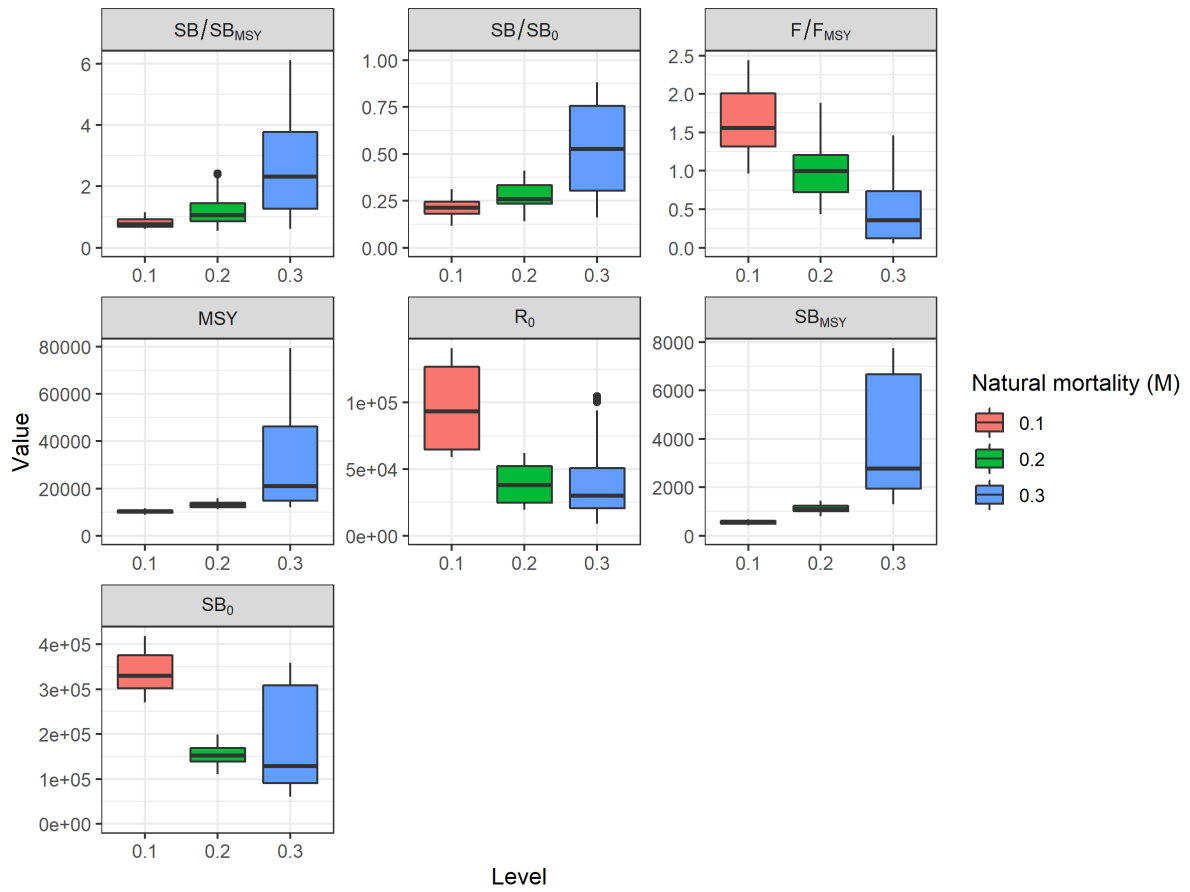


Figure 4. Boxplots of the estimated stock status (SB/SB_{MSY} , SB/SB_0 , and F/F_{MSY}) and estimated reference points (MSY , R_0 , SB_{MSY} , SB_0) for the 216 operating models in the uncertainty grid, with colors indicating the three levels in the axes for natural mortality rate (M).

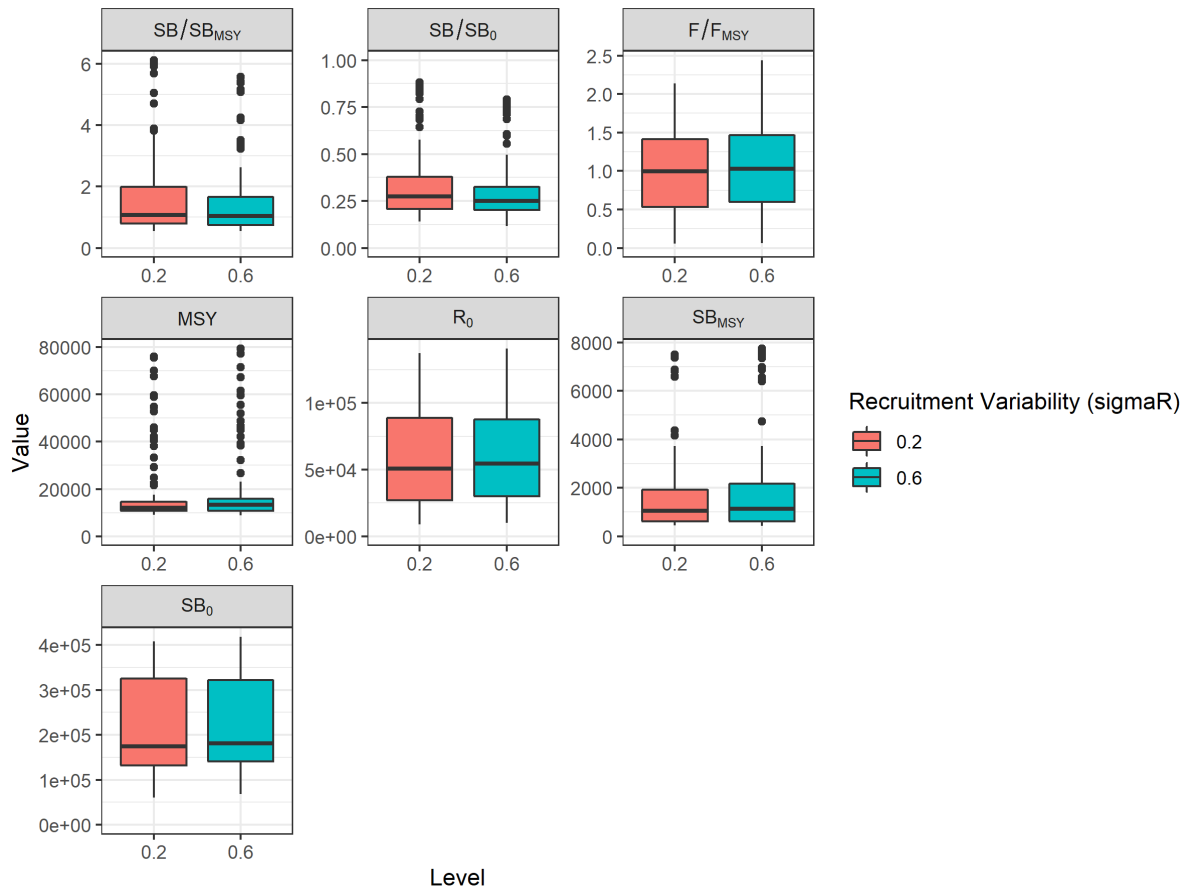


Figure 5. Boxplots of the estimated stock status (SB/SB_{MSY} , SB/SB_0 , and F/F_{MSY}) and estimated reference points (MSY , R_0 , SB_{MSY} , SB_0) for the 216 operating models in the uncertainty grid, with colors indicating the two levels in the axes for recruitment variability (σ_R).

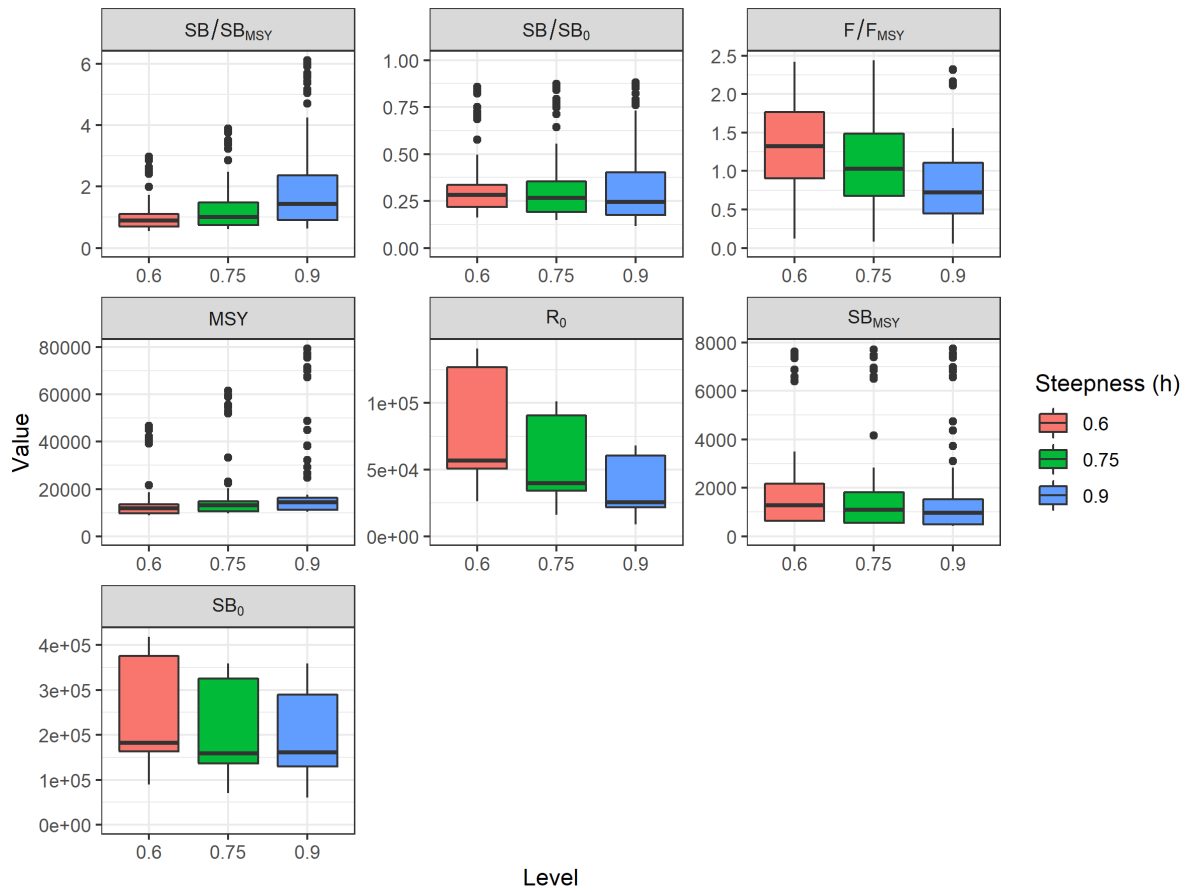


Figure 6. Boxplots of the estimated stock status (SB/SB_{MSY} , SB/SB_0 , and F/F_{MSY}) and estimated reference points (MSY , R_0 , SB_{MSY} , SB_0) for the 216 operating models in the uncertainty grid, with colors indicating the three levels in the axes for steepness (h).

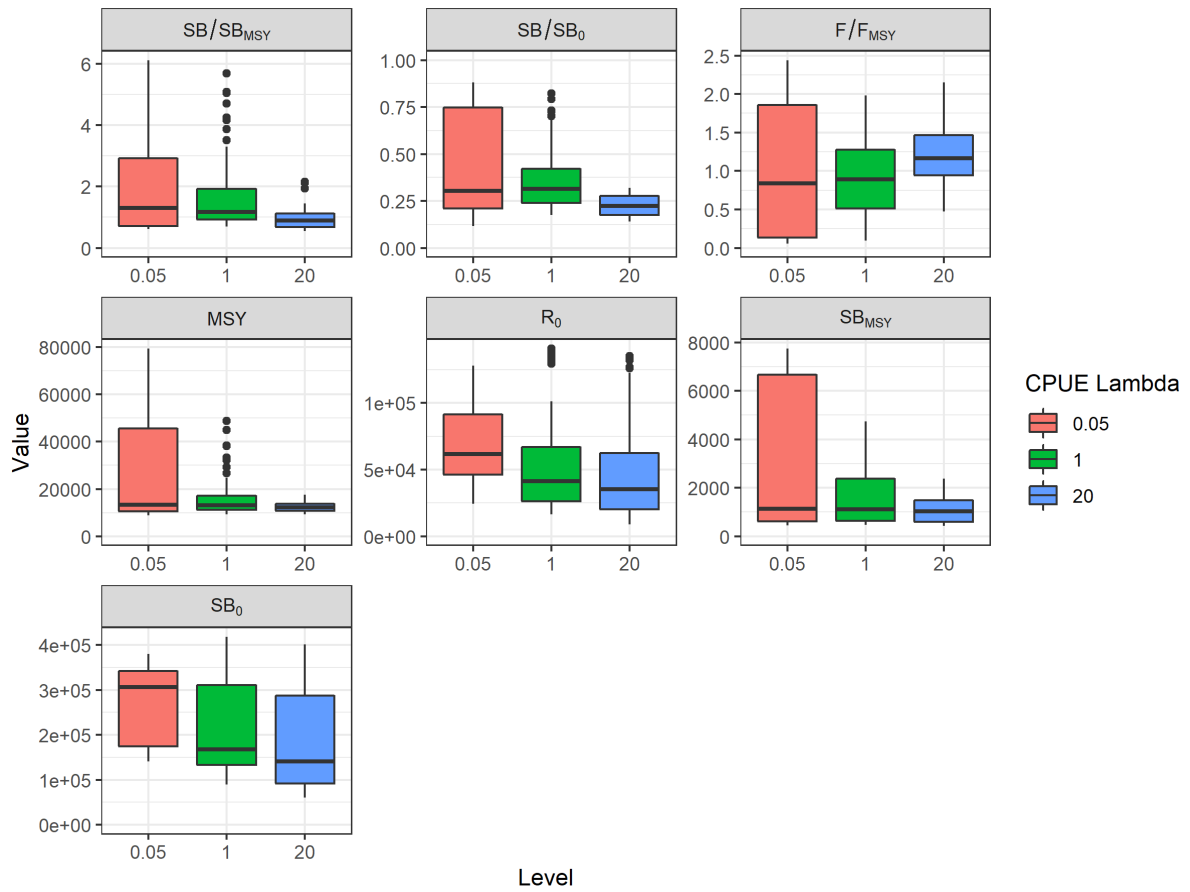


Figure 7. Boxplots of the estimated stock status (SB/SB_{MSY} , SB/SB_0 , and F/F_{MSY}) and estimated reference points (MSY , R_0 , SB_{MSY} , SB_0) for the 216 operating models in the uncertainty grid, with colors indicating the three levels in the axes for the lambda of the CPUE indices.

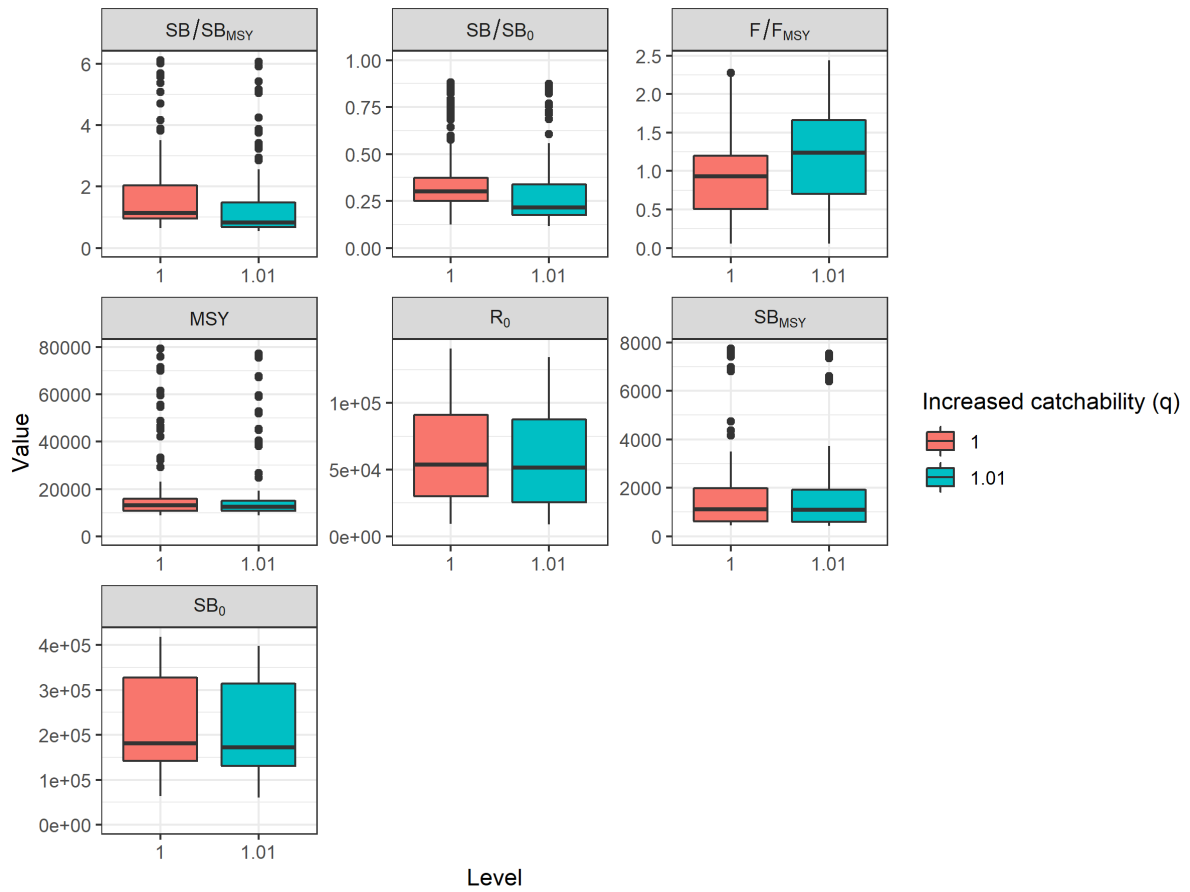


Figure 8. Boxplots of the estimated stock status (SB/SB_{MSY} , SB/SB_0 , and F/F_{MSY}) and estimated reference points (MSY , R_0 , SB_{MSY} , SB_0) for the 216 operating models in the uncertainty grid, with colors indicating the two levels in the axes for the assumed 1% annual increase in catchability.

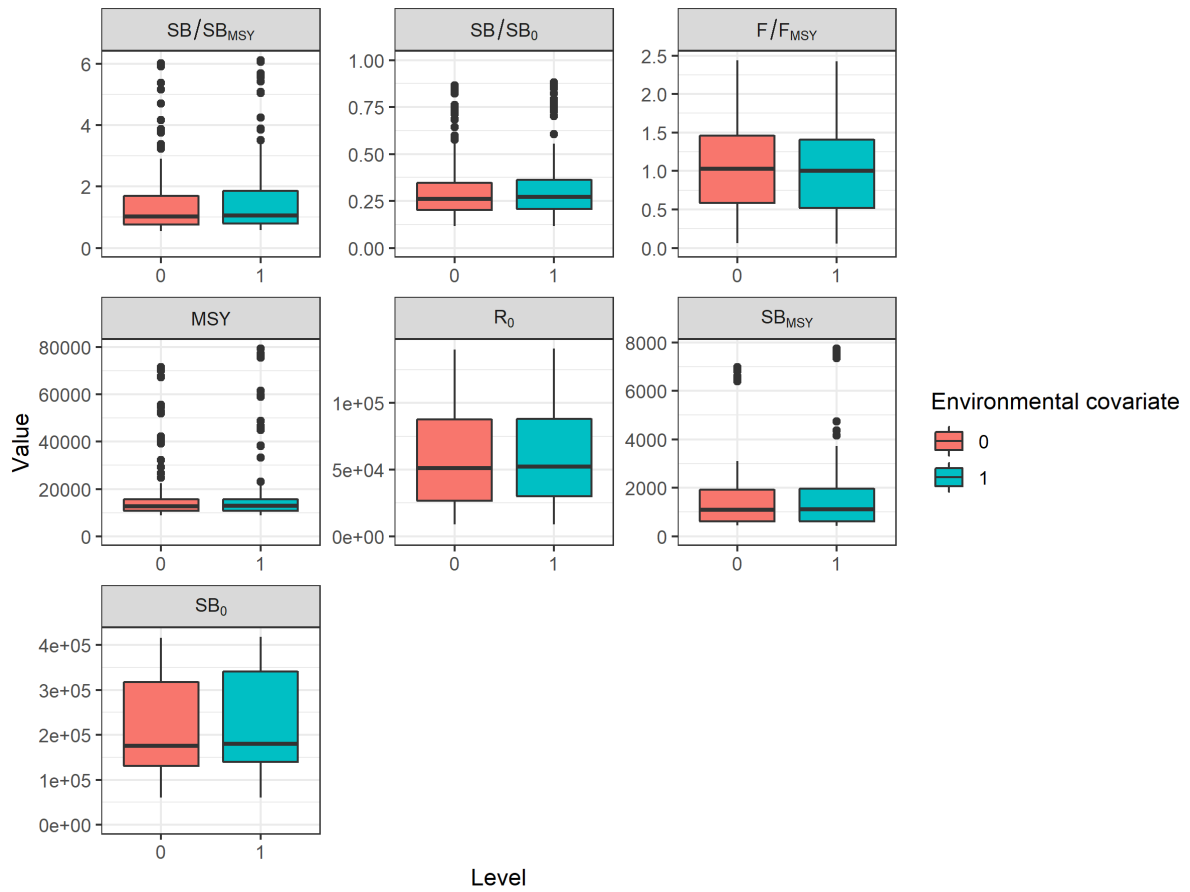


Figure 9. Boxplots of the estimated stock status (SB/SB_{MSY} , SB/SB_0 , and F/F_{MSY}) and estimated reference points (MSY , R_0 , SB_{MSY} , SB_0) for the 216 operating models in the uncertainty grid, with colors indicating the two levels in the axes for the assumed environmental covariate with the CPUE indices.

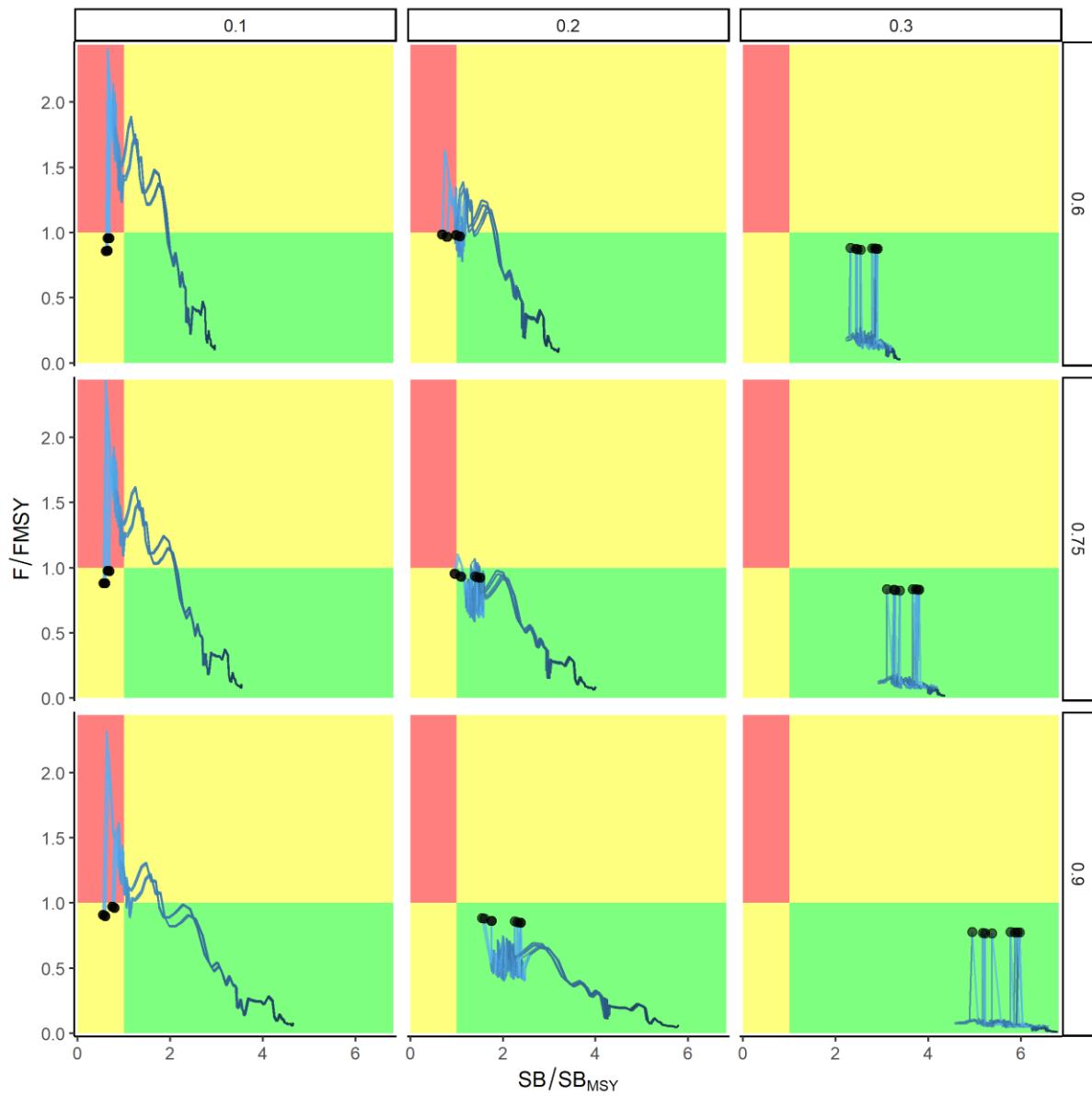


Figure 10. Bi-variate Kobe plots for the three levels of steepness (rows) and three levels of natural mortality (columns) for the 72 operating models where CPUE lambda was 0.05 (lambda for the length composition data was 1). The lines are shaded from dark (beginning of time-series) to light (end of time-series) with the black point indicating the estimates from the terminal year (2017).

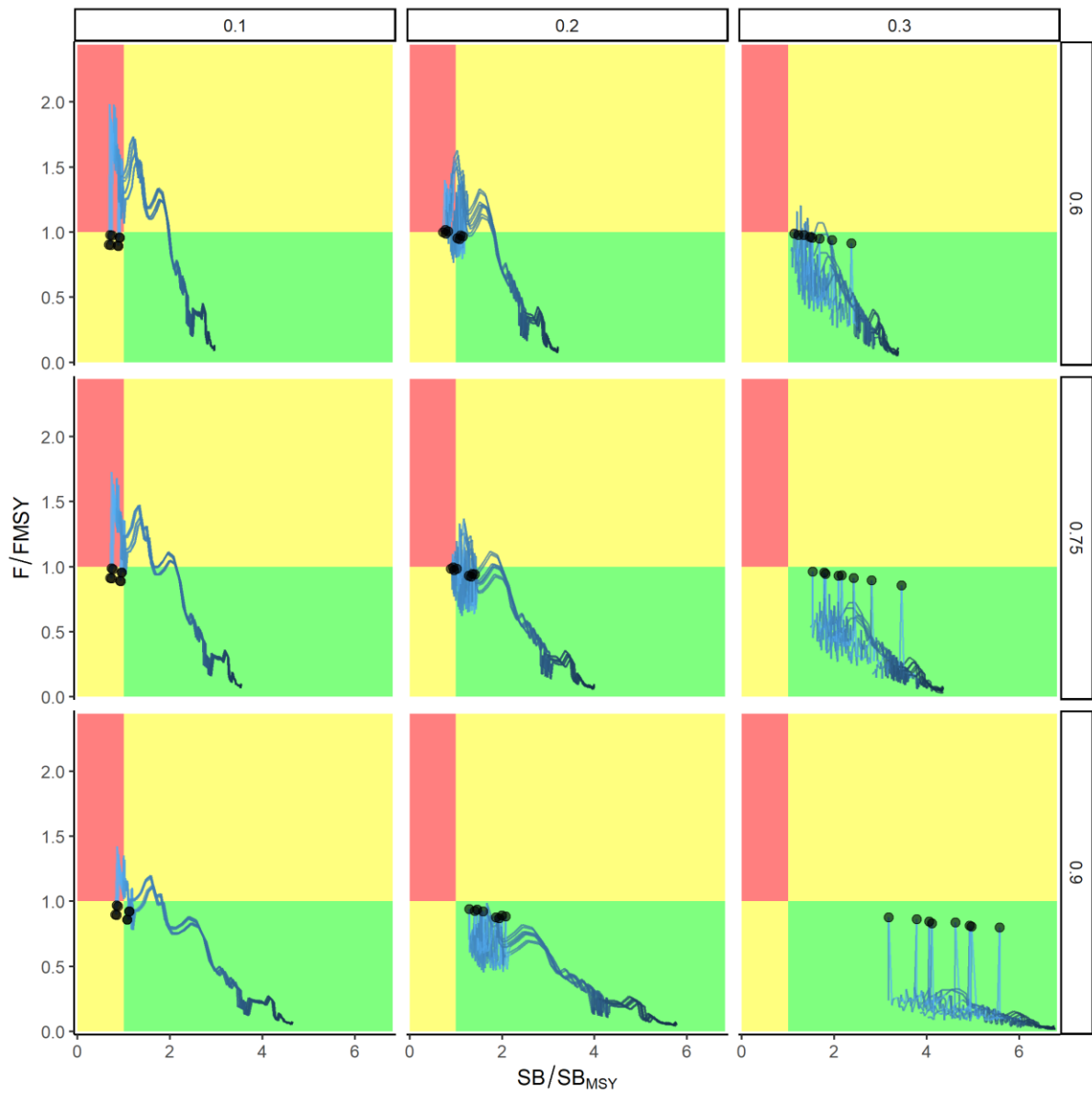


Figure 11. Bi-variate Kobe plots for the three levels of steepness (rows) and three levels of natural mortality (columns) for the 72 operating models where CPUE lambda and lambda for the length composition data were both 1. The lines are shaded from dark (beginning of time-series) to light (end of time-series) with the black point indicating the estimates from the terminal year (2017).

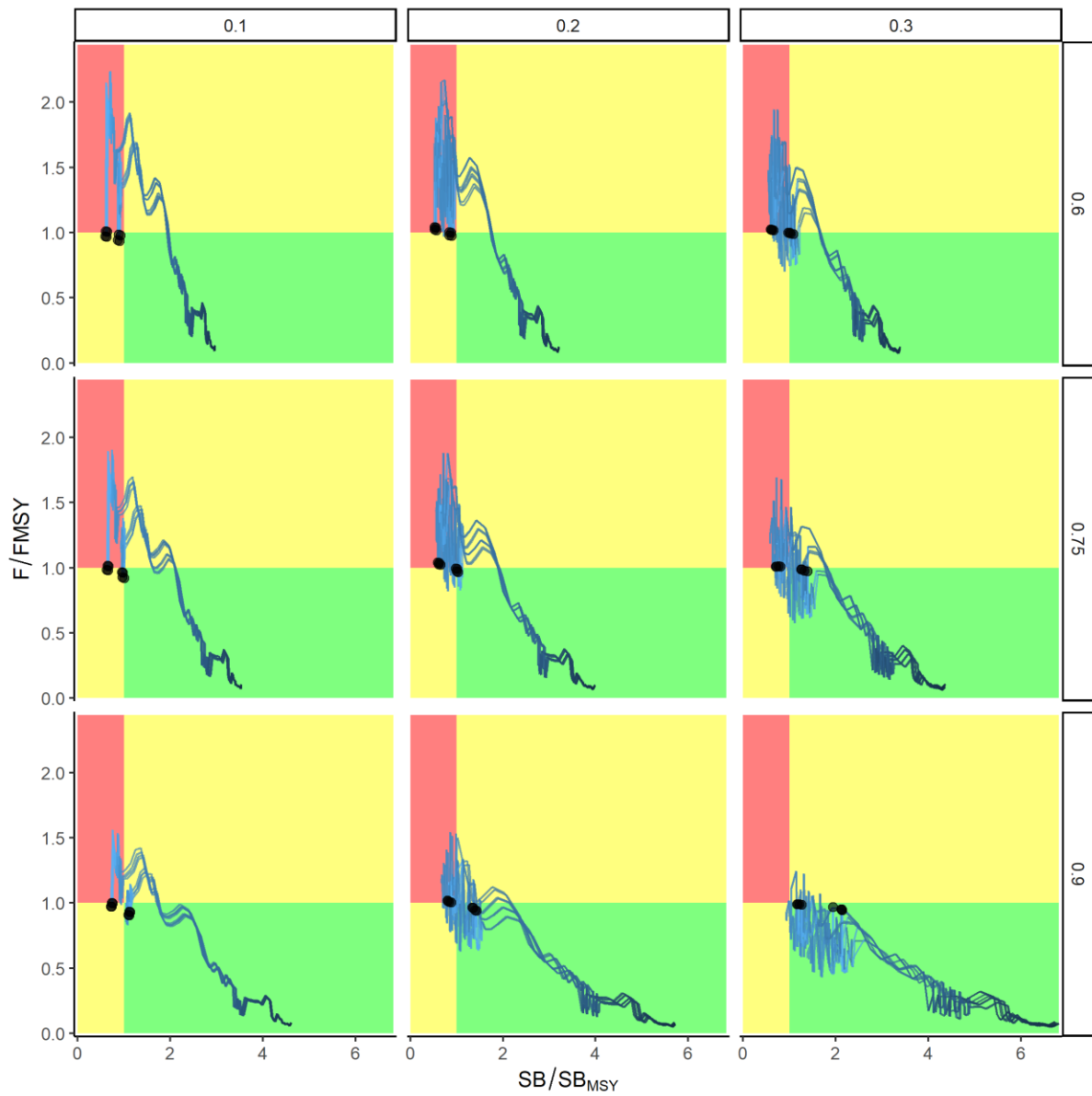


Figure 12. Bi-variate Kobe plots for the three levels of steepness (rows) and three levels of natural mortality (columns) for the 72 operating models where CPUE lambda was 20 (lambda for the length composition data was 1). The lines are shaded from dark (beginning of time-series) to light (end of time-series) with the black point indicating the estimates from the terminal year (2017).

9 Appendices

9.1 Appendix A

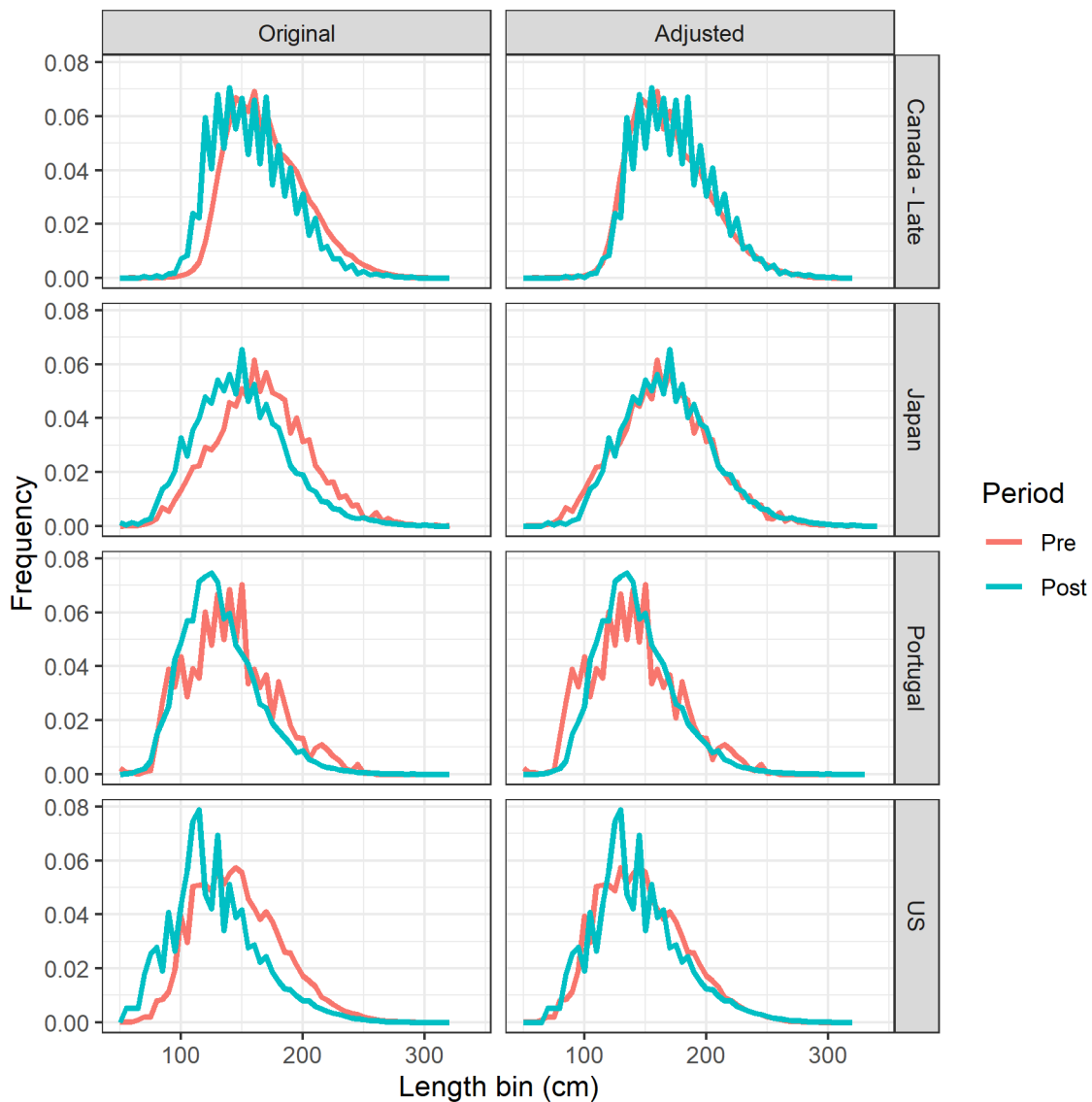


Figure A1. The Original (left column) and Adjusted (right column) length frequency data before 1993 (Pre; red) and from 1993 – 2017 (Post; blue) for the Canada –Late, Japan, Portugal, and US fleets. The Original length frequencies from the Post period appeared to be shifted to the left of the Pre data by 2 – 4 length bins. The Adjusted length data fixes this apparant issue by shifting the Post length frequency data so that the ascending limb and peaks match those from the Pre period. The Adjusted length data was used in the OM conditioning reported in this paper.

9.2 Appendix B

9.2.1 Individual OM Diagnostic Reports

Detailed reports on the objective function values, fits to CPUE indices and length composition data, and plots of the estimated stock status and biological reference points for the 216 operating models are available on the North Atlantic Swordfish MSE homepage (<https://iccat.github.io/nswo-mse/>).

9.2.2 Additional Summary Plots

Additional summary plots of the OM dynamics, including time-series plots of SB/SB_{MSY} , F/F_{MSY} , and correlation plots of the levels within each factor can be found in the online appendix (https://iccat.github.io/nswo-mse/Reports/OM_Summary/SCRS_2021_090_Appendix_B.html).